Hydrothermal carbonization and pyrolysis of sewage sludges: ~~w~~What happen to carbon and nitrogen?

M. Paneque[a,*]

mpaneque@irnas.csic.es

J.M. De la Rosa[a]

J. Kern[b]

M.T. Reza[c]

H. Knicker[a]

[a]Instituto de Recursos Naturales y Agrobiología de Sevilla (IRNAS-CSIC), Reina Mercedes Av. 10, 41012, Seville, Spain

[b]Leibniz-Institut für Agrartechnik and Bioengineering, Max-Eyth-Allee 100, 14469 Potsdam, Germany

[c]Department of Mechanical Engineering, 1 Ohio University, Athens, OH 45701, USA

[*]Corresponding author.

Abstract

Hygienization by thermochemical carbonization may be one option to enable the use of sewage sludge (SS) as soil amendment and nitrogen (N) fertilizer. To evaluate this possibility, SS derived from different water purification processes of a rural waste water treatment plant were hydrothermal carbonized (HTC) at 200 and 260 °C for 0.5 and 3.0 h, and pyrolyzed at 600 °C for 1 h. During HTC, temperature rather than residence time affected the chemical alteration. Solid-state ^{13}C and ^{15}N nuclear magnetic resonance (NMR) spectroscopy showed considerably lower aromaticity in the hydrochars than in the pyrochars. Whereas the aromatic network of the hydrochars is dominated by polyfurans and N-heterocyclic aromatic units that of the pyrochars is mainly composed of arene structures. The highest total and inorganic N contents were obtained via HTC at 200 °C for 30 min, thus this material may be applied if both immediate and slow N release is needed.

Keywords: Slow-release N fertilization; Hygienization; Pyrochar; Hydrochar; Solid-state NMR spectroscopy

1 I~~NTRODUCTION~~ntroduction

In the European Union (EU), the major N and P sources in agriculture are synthetic fertilizers although inputs from animal manure remain important, especially in regions of high livestock density. The use of synthetic fertilizers has dramatically increased food production worldwide, but the unintended costs to the environment and human health due to surplus and inefficient application have also been substantial. Thus, alternatives are needed. One of those represents the valorization of organic waste, the amount of which increased exponentially during the last decades. Its estimated annual increase is around 25 million tons [1].

A major source of organic waste is sewage sludge (SS). Containing high amounts of N, with a median of 3.3% [2], P and OM, this material offers an excellent feedstock for the production of soil amendments that can reduce the need of synthetic P and N fertilizer [3,4]. At the same time it may increase the C-sequestration potential of cropped soils. In addition, sludge recycling as fertilizer or organic amendment helps to reduce the amount of organic waste by returning it into the bio-cycle while at the same time soil physical and chemical properties are restored [5,6]. Indeed, the Sewage Sludge Directive [7] and the working document on sludge [8] describe the use of SS on soils as beneficial but also seek to encourage a safe use of this material in agriculture and to regulate its application to prevent harmful effects on soil, vegetation, animals and humans [9]. Thus, in order to enable the use of SS as soil application, it first has to be decontaminated by removing organic pollutants and pathogen bacteria. Different treatments can be used for the latter: thermal drying, anaerobic digestion, conditioning with lime, etc. In general, the process of removing pathogen bacteria of SS is called hygienization. Heavy metals content also need to be taken into account. In cases their concentrations are above the allowed thresholds, strategies have to be developed to avoid secondary contamination due to SS application.

The thermochemical carbonization of SS at elevated temperatures in the absence of oxygen has recently been considered to achieve sludge stabilization and hygienization. In the presence of water, this kind of carbonization is called hydrothermal carbonization (HTC), whereas in the absence of water it is known as pyrolysis. During pyrolysis, temperatures between 300– and 700 °C are used [10]. The solid product is considered as biochar, according to the European Biochar Foundation, if it derives from a feedstock approved for this organization, its organic carbon content is above 50% and its atomic H/C ratio is <0.7 [11]. Considering that these thresholds are rarely reached with carbonized SS, in the following we refer to pyrolyzed SS as pyrochar. Hydrochars represent the solid residue after heating biomass together with water at 180–250°–250 °C for 1–12 h under autogenous pressure [12]. Due to the high humidity of SS, the application of HTC avoids the necessity of an additional drying step. Both types of carbonization include reactions such as dehydration, decarboxylation, aromatization and recondensation [13,12]. However, the different process conditions lead to significant differences of both the chemistry and physical characteristics of the solid products [12]. Accordingly, hydrochars contain a high amount of furan-type structures. On the other hand, pyrochars produced at high temperatures are composed of an arene-rich core [14–16].

Despite alterations of the organic C fraction during the pyrolysis and HTC of biomass have already been focus of many investigations [10,17–19] the knowledge about changes of organic N is still scarce. Previous studies have shown that after incomplete combustion of N-rich plant residues and casein at 350 °C for several minutes a considerable part of their organic N was incorporated into heterocyclic aromatic structures, the so called pyrogenic organic nitrogen [20,21]. Although this nitrogen is less bio-available than mineral fertilizer it was mobilized and used by plants and microbes for the neo-formation of biomass and amides [22]. Thus, N-rich carbonized OMs may be prime candidates for the development of slow N-release fertilizers, since the mobilization of their N is expected to be sufficiently low to avoid fast N losses due to leaching or nitrification shortly after fertilizer application. A deeper knowledge of the N transformations during the thermochemical carbonization of SS is necessary in order to evaluate its potential to fulfill this function. Wei et al. [23] found that ammonia (NH_3) is the main product of protein-N during SS pyrolysis and that the majority of pyridine N originally present in SS tends to be converted into hydrogen cyanide (HCN) at 400–600 °C. Studying HTC as a potential tool to reduce NH_3 and HCN emissions during the pyrolysis of SS-derived residues, Liu et al. [24] confirmed the conversion of nitrogen into more stable forms by the application of HTC.

Since chemical composition and physical properties of a soil amendment define its function, the goal of the present research was a detailed characterization of the chemical changes during HTC and pyrolysis of two different SS. This analysis was not limited to the organic C fraction but included also the N-forms. The SS used in this study derived from a rural waste water treatment plant of a community with approximately 3000 inhabitants. They were collected from an extensive and an intensive cleaning process. It is important to bear in mind that physical and chemical properties of the SS depend on the wastewater treatment process by which it was produced and on the characteristics of the treated effluents [25]. For example, the commonly called primary SS is formed from suspended organic material which is separated by sedimentation; whereas secondary sludge constitutes mainly residues of bacteria biomass which is involved in the digestion of the easily metabolized organic fraction of the water. Thus, primary sludge is expected to be biochemically less stable than secondary sludge [5]. This may also affect the chemical alteration during thermal carbonization, which was applied for hygienization before it can be applied as soil amendment. In order to evaluate the potential of the products as slow-release N fertilizer, their chemical structures was not only analyzed by Infrared (IR-FT) and solid-state ^{13}C NMR spectroscopy but also by solid-state ^{15}N NMR spectroscopy. Preliminary analysis confirmed that heavy metal contents of the products were below allowed thresholds. With the approach used for this study and as known to the authors, we were able to obtain the first solid-state ^{15}N NMR spectra of hydrochars.

2 M~~ATERIALS AND METHODS~~aterials and methods

2.1 Sewage sludge

Two different SS were collected at the Experimental Wastewater Treatment plant (CENTA), located in Carrion de los Céspedes, within the province of Seville (Spain). This plant processes the domestic wastewater of the village with over 3000 residents. The experimental nature of this plant allows treating the wastewater by using different intensive and extensive technologies.

The first sample, A_SS, is a primary sludge produced after the settlement of suspended OM and its subsequent anaerobic digestion in a pond. The long residence time of five to ten years, promote stabilization of the remaining OM.

The second sample, T_SS, is a secondary sludge produced in an extended aeration treatment system and later stored in a thickener in order to reduce its water contents. However, due to the long residence time of the sludge in the thickener, part of the organic matter can be further mineralized and humified.

2.2 Production of chars

Considering the high amount of water in sewage sludge, we focused on the study of the HTC effect since this technique avoids the necessity of an additional drying step. However, we also produced two samples by using pyrolysis for comparison.

For the production of hydrochars 1 L-stirred pressure reactor (Parr reactor series 4520, IL, USA) equipped with an external resistance heater and internal sensors for pressure and temperature was used and the material was

heated at 200 °C and 260° C for 30 min and 3 h with a heating rate of 3 °C min^{-1}. For each temperature and time, 225 g of SS were mixed with 450 g of distilled water and placed into the reactor. During HTC, the mixture was stirred at a constant speed of 90 rpm. The reactor required approximately 120 min to reach the desired temperatures. The temperatures were maintained at the set-point during the whole reaction time after which the heater was turned off and the heat insulation was removed. A hooked-shaped agitator stirred the sludge water mixture with a rotation velocity of 90 rpm. After cooling for approximately 15 h, the HTC slurry was filtered through fluted filter paper and the solids were dried for 48 h at 60 °C.

For the production of the pyrochars, 200 g of dry SS were placed into a close steel container and heated in a preheated muffle oven at 600 °C for 1 h.

2.3 Chemical composition

The dry-weight of the samples after pyrolysis was determined after drying at 105 °C, the ash content after heating at 750 °C for 5 h. The pH values were measured in distilled water (1:2.5, w/v). Hydrogen (H), C and N contents were obtained with an elemental analyzer (Vario EL III, Elementar Analysensysteme, Germany). The amount of oxygen (O) was calculated by difference. For the analysis of plant available N ammonium (NH_4^+) and nitrate (NO_3^-), those N-components were extracted with 0.0125 M $CaCl_2$ (5 ml g^{-1} dry sample) and measured by flow-injection analysis (FIA System, MLE, Germany).

2.4 Solid state ^{13}C and ^{15}N ~~Nuclear Magnetic Resonance S~~nuclear magnetic resonance spectroscopy

Prior to the solid-state NMR spectroscopy, the SS and the chars were subjected to four successive treatments with 10% (m/m) hydrofluoric acid (HF) to increase the organic matter concentration by removing minerals and paramagnetics. After discarding the supernatant, the solid residue was rinsed with distilled water until a pH-value >5 was yielded and finally freeze-dried [26].

The solid-state ^{13}C NMR spectra were obtained with a Bruker Avance III HD 400 MHz WB spectrometer, using a triple resonance broadband probe and zirconium rotors of 4 mm OD with KEL-F-caps. The cross polarization (CP) technique was applied during magic-angle spinning (MAS) of the rotor at 14 kHz. A ramped ^1H-pulse was used during a contact time of 1 ms to circumvent Hartmann-Hahn mismatches. Pre-experiments confirmed that a pulse delay of 300 ms was long enough to avoid saturation. Between 5000 and 13,000 scans were accumulated for each sample, and the line broadening was between 50 and 100 Hz. The ^{13}C chemical shift scale was calibrated relative to tetramethylsilane (0 ppm) with glycine (COOH at 176.08 ppm). The relative ^{13}C intensity distribution was determined by integrating the following chemical shift regions: alkyl C (0–45 ppm); *N*-alkyl/methoxyl C (45–60 ppm); *O*-alkyl C (60–90 ppm); anomeric C (90–110 ppm); aryl C (110–140 ppm); *O/N*-aryl C (140–160 ppm); carboxyl/amide C (160–220 ppm).

For none of the samples, the atomic H/C ratio was below 0.5 indicating that the protonation degree was sufficiently high for efficient cross polarization. Thus the intensity distribution of the spectra is comparable to the chemical composition of the organic matter of the sample. Note that in highly aromatic samples the region commonly assigned to anomeric C is dominated by resonances from aromatic structures. At a spinning speed of 14 kHz the chemical shift anisotropy is not completely averaged, which causes spinning side bands appearing at both sides of the parent signal at a distance of the spinning speed (here between 250 and 300 ppm and between −50 and 0 ppm). Their intensity was added to the region of the parent signal.

The solid state ^{15}N NMR spectra were obtained using the same instrument but a 7 mm double resonance probe and operating at 40.56 MHz. The contact time was 1 ms. A 90°H pulse width of 3.5 µs, a pulse delay of 200 ms and a line broadening between 50 and 100 Hz were applied. Between 300.000 and 2 millions of scans were accumulated at a MAS speed of 6 kHz. The chemical shift was standardized to the nitromethane scale (0 ppm) and adjusted with ^{15}N-labelled glycine (~~-~~347.6 ppm). The following chemical shift regions were integrated: amide N (~~-~~248 to −285 ppm) and pyrrole N (~~-~~150 to −248 ppm).

In order to obtain more insights into the chemical alterations occurring during pyrolysis, the recovery of organic C in each C group in the respective char as a function of treatment Cx (hc) was calculated according to ~~equation~~ Eq. (1):

$$Cx\ (hc) = \frac{C\ (x)\ *\ C\ (t)}{100} \quad \textbf{(1)}$$

Here, C (t) is the remaining C in the hydrochar in % of the C content of the original SS (Cs), C(x) is the relative ^{13}C intensity of a ^{13}C chemical shift region.

2.5 Fourier-~~Transform I~~transform infrared spectroscopy (FT-IR)

The FT-IR spectra were recorded using a JASCO 4100 spectrometer at wavenumber ranging from 4000 to 400 cm^{-1} and a resolution of 2 cm^{-1}. Potassium bromide pellets containing about 1% (w/w) of each biochar were prepared in a cylindrical piston under high pressure and vacuum. In order to improve the signal-to-noise ratio, 60 scans were registered and accumulated for each recorded spectrum. The spectra were corrected against a spectrum of pure KBr pellet prior to every measurement. All IR data manipulations were performed using JASCO spectra manager software® (Japan).

3 R~~ESULTS AND DISCUSSION~~esults and discussion

3.1 Weight loss and alteration of the composition during carbonization

3.1.1 Mass loss during charring

Among the applied treatments, pyrolysis at 600 °C resulted in the lowest yields, which accounted for 71 and 65% of the original dry weight for the pyrochars from A (A_Py_600_1) and T (T_Py_600_1), respectively (Table 1). Yields after HTC ranged between 87 and 73%. Whereas an increase of the residence time did not change the yields, augmentation of the temperature from 200 °C to 260 °C resulted in a slight increase of the mass loss. Compared to our recoveries of 87 and 83% for A_HTC_200_0.5 and T_HTC_200_0.5 respectively, Danso-Boateng et al. [27] reported considerably lower values of 67% of the initial mass after HTC of primary SS at comparable conditions. This may be best explained by the different biochemical stability of the feedstock, which remarks the importance to consider the SS production conditions for the discussion and extrapolation of HTC characteristics.

Table 1 Weight recovery after the thermal treatment of primary (A_SS) and secondary (T_SS) sewage sludges, the ash contents, the elemental composition (C, N, O, S, H) and the recovery for the respective hydrochars produced at 200 °C (_HTC_200) and 260 °C (_HTC_260) for 0.5 and 3 h~~ours~~ (_0.5, _3, respectively, as well as the pyrochars produced at 600 °C for 1 h (_Py__600_1).

alt-text: Table 1

			Elemental composition				Recovery with respect to the untreated sample			
Sample	Weight Recovery	Ash content	C	N	O[b]	H	C	N	O	H
	% DM[a]	mg g^{-1}	mg g^{-1}	mg g^{-1}	mg g^{-1}	mg g^{-1}	% DM	% DM	% DM	% DM
A_SS	100	540	228	19	168	34	100	100	100	100
A_HTC_200_0.5	87	611	224	16	108	30	85.1	72.4	55.5	75.2
A_HTC_200_3	87	625	214	14	110	27	81.2	62.9	56.3	68.0
A_HTC_260_0.5	82	656	213	11	82	26	76.9	48.0	40.3	63.2
A_HTC_260_3	82	657	221	12	72	27	79.1	51.6	35.0	63.9
A_Py_600_1	71	761	134	9	82	9	41.6	32.0	34.6	18.6
T_SS	100	507	245	32	167	37	100	100	100.0	100
T_HTC_200_0.5	83	570	233	25	128	30	79.0	64.3	64.1	66.0
T_HTC_200_3	79	612	233	24	89	27	75.1	58.5	42.0	58.0
T_HTC_260_0.5	76	645	225	20	69	26	69.5	46.2	31.1	52.6
T_HTC_260_3	73	661	224	19	57	25	66.7	42.9	24.9	49.7
T_Py_600_1	65	726	168	16	70	9	44.6	32.9	27.3	16.3

[a] DM: dry matter.

[b] ~~c~~Calculated by difference.

3.1.2 Ash content

Approximately half of the untreated A and T SS is composed of ash (Table 1). These results are comparable with those obtained by Zielinska et al. [25]. The ash in the SS sample probably derives from the contribution of street wastewater run offs into the wastewater collecting system and from the sand used during the mechanical pre-treatment of the water-cleaning process. Charring leads to dehydration and loss of OM, which increases the relative content of ash in the respective chars. The highest ash contents were determined for the samples A and T pyrolyzed at 600 °C under dry conditions (761 and 726 mg g^{-1} respectively; Table 1).

3.1.3 Elemental composition (C, H, N, O)

The total C content of the non-treated SS is <250 mg g^{-1}. Whereas between 85 and 67% of the organic C in the SS survived HTC, pyrochars contained only 42 and 45% of the initial amount of C (Table 1). This is explained by a more efficient incomplete carbonization during pyrolysis compared to HTC [12]. Compared to wood-derived biochars which C contents >500 mg g^{-1}, the low carbon concentration of both, the original SS and the chars may limit their use if only an enhancement of the carbon sequestration potential of soils is wanted. Compared to C yields after charring, the O and H recoveries are lower, which reflects ongoing dehydratation, dehydroxylation, decarboxylation and condensation. This is confirmed in the Van Krevelen diagram (Fig. 1) which shows a decrease of atomic H/C and O/C ratios as carbonization enhances. Note that all hydrochars depict atomic H/C values >1. Thus, in average, each C atom is directly bound to at least one H, which opposes a highly condensed aromatic structure [28,29]. On the other hand, the pyrochars exhibit values of 0.7 and 0.8, which assigns each 1.5C to one hydrogen, allowing aromatics condensed structures with maximal six rings in average. These results are within those expected according to bibliography [30–32].

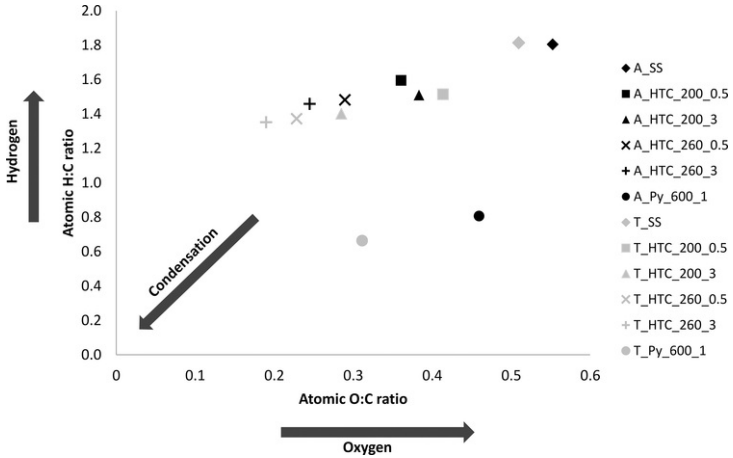

Fig. 1 van Krevelen diagram of primary (A_SS) and secondary (T_SS) sewage sludges and their respective hydrochars produced at 200 °C (_HTC_200) and 260 °C (_HTC_260) for 0.5 and 3 h~~ours~~ (_0.5, _3, respectively), as well as the pyrochars produced at 600 °C for 1 h (_Py__600_1)

alt-text: Fig. 1

The total N content of A_SS and T_SS are 19 and 32 mg g^{-1}, respectively (Table 1). These values are within the range reported for this material [33]. Compared to C, higher losses of N were observed for both hydrochars and pyrochars. However, in all the charred samples the N contents are still >9 mg g^{-1}, most of which occurs in organic forms (>97%) (Table 2). Therefore, the organic N sequestered in these chars is likely to affect the N cycling in soils once this material has been applied. The bioavailability of organic N in the chars is influenced by its composition and by the chemical and biological changes it undergoes after its addition to soil, but still, it will be lower than that expected for inorganic N forms (N_i). After all charring treatments, the C_{org}/N ratio (w/w) increased slightly, most tentatively due to deamination and degradation of amino acids and amino sugars, but also by volatilization of NH_3 and nitrous oxides. However, even after inclusion the pyrochars, the C/N ratios do not exceed the value of 20, which is considerably lower than biochars from wood [31]. Thus, if the organic N in chars occurs in bioavailable forms, both the hydro- and pyrochar can serve as an efficient additional N-source for biomass production provided sufficient bioavailable C is present, too.

Table 2 pH, C_{org}/N ratios, and inorganic nitrogen (N_i) contents of primary (A_SS) and secondary (T_SS) sewage sludges and their respective hydrochars produced at 200 °C (_HTC_200) and 260 °C (_HTC_260) for 0.5 and 3 h~~ours~~ (_0.5, _3, respectively), as well as the pyrochars produced at 600 °C for 1 h (_Py__600_1).

alt-text: Table 2

Sample	pH	C_{org}/N	NH_4-N	NO_2-N	NO_3-N	N_i[a] of the total N
		(w/w)	mg kg^{-1}	mg kg^{-1}	mg kg^{-1}	%
A_SS	7.4	11.9	115	0.03	0.18	0.5
A_HTC_200_0.5	6.5	14.0	417	0.36	0.59	2.6
A_HTC_200_3	6.5	15.4	349	0.20	0.34	2.5

A_HTC_260_0.5	6.4	19.1	169	0.06	0.15	1.5
A_HTC_260_3	6.6	18.2	227	0.05	0.003	1.9
A_Py_600_1	9.3	15.5	0.2	0.003	–[b]	0.0
T_SS	7.5	7.6	123	0.04	0.57	0.4
T_HTC_200_0.5	6.7	9.3	542	0.76	1.26	2.2
T_HTC_200_3	6.2	9.7	341	0.36	0.44	1.4
T_HTC_260_0.5	6.3	11.4	239	0.09	0.47	1.2
T_HTC_260_3	6.4	11.8	256	0.04	–	1.4
T_Py_600_1	10.0	10.3	0.3	–	–	0.0

[a] N_i: sum of NH_4-N,NO_2-N, and NO_3-N in ~~%.b~~ %.

b –: below the detection limit.

The contribution of N_i to total N increased after HTC from 0.5 to 2.6% and from 0.4 to 2.2% for A and T hydrochars, respectively. However, after pyrolysis all N_i was lost (Table 2). Regarding the different available inorganic nitrogen forms, for both A_SS and T_SS the NH_4-N contents are considerably higher (115 and 123 mg kg^{-1}, respectively) than their NO_2-N and NO_3-N contributions. This trend was also observed by Alvarenga et al. [34], Adegbidi and Briggs [35] and Hossain et al. [36]. Increasing NH_4-N levels after HTC at 200 °C are best explained with deamination reactions. Increasing the temperature leads to further transformation and to N losses into the gaseous phase. Here, one has to bear in mind that the liquid phase which was discarded can represent a further considerable sink for inorganic N. Comparable trends, but at a much lower concentration level, are observed for NO_2-N and NO_3-N. The increase of NH_4^+ after HTC is in agreement with the results obtained by Sohn and Ho [37], who demonstrated that after heating aqueous solutions of amino acids at 180 °C during 2 h, considerable amounts of NH_3 were released. On the other hand, Jin-hong et al. [38] reported a considerable decrease of available NH_4-N and NO_3-N for SS hydrochars produced at 190 and 260° C during 1, 6, 12, 18 and 24 h. They may have achieved the lack of N_i in their samples because of intense rinsing of the HTC-chars with distilled water. Thus, post-treatment processes also need to be taken into account to evaluate the fertilizer potential of HTC chars. Here one has to bear in mind that efficient removal of N_i may counteract fertilization purpose since this easily available N form would be accessible already during the early plant growing stage.

In contrast to the HTC chars, the pyrochars did not accumulate N_i and consequently, their remaining N must have been sequestered in organic constituents of the char as it was suggested by Knicker [21]. Thus, whereas pyrolysis turns almost the entire liberated N into gaseous compounds HTC leads to deamination and accumulation of NH_4^+. However, some of the N will be also lost through the liquid phase.

3.2 Solid-state ^{13}C and ^{15}N NMR spectroscopy

3.2.1 Sewage sludge materials

The solid-state ^{13}C NMR spectra of both A_SS and T_SS are dominated by signals in the chemical shift region of alkyl C (0–45 ppm). Both lipids and peptides can contribute to this region, which comprises 43 for A_SS and 38% for T_SS of the total ^{13}C signal intensity (Table 3). Their carboxyl C and amide C add to the signal at 174 ppm in the chemical shift region between 220 and 160 ppm (Fig. 2). The *O*-alkyl C region (90–60 ppm) accounts for 17 and 23% of the total ^{13}C intensity for A_SS and T_SS, respectively. The latter comprises signals from C2-C5 in carbohydrates, alcohols and ethers. The region between 110 and 90 ppm is commonly assigned to anomeric C (C1) in pentoses and hexoses but can also derive from C2 and C6 in lignin derivatives. However, lignin compounds are of minor importance in SS, which is mainly composed of proteins, carbohydrates, fats and oils [6]. In addition, A_SS contains slightly more aromatic C (160 ~~to~~ –110 ppm) than T_SS. Considering the low contribution of lignin to SS, most of this signal intensity derives from aromatic amino acids or olefinic structures, which contribute to this chemical shift region, too. Jin-hong et al. [38] showed also a dominance of the alkyl C region for SS, with a value of 64%. This is due to the large contribution of fat acids but also peptides typically present in domestic SS [6].

Table 3 Intensity distribution (%) of the solid-state ^{13}C NMR spectraof primary (A_SS) and secondary (T_SS) sewage sludges and their respective hydrochars produced at 200 °C (_HTC_200) and 260 °C (_HTC_260) for 0.5 and 3 h~~ours~~ (_0.5, _3, respectively), as well as the pyrochars produced at 600 °C for 1 h (_Py__600_1).

alt-text: Table 3

	Carboxyl/Amide C	O/N- Aryl C	Aryl C	O-Alkyl C	N-Alkyl/Methoxyl C	Alkyl C	Alkyl C/Carboxyl C	Alkyl C/O-Alkyl C

ppm	220–160	160–140	140–110	110–90	90–60	60–45	45–0		
A_SS	9.1	2.8	10.4	4.3	17.3	12.9	43.1	4.7	2.5
A_HTC_200_0.5	6.3	5.0	16.3	3.6	12.0	9.6	47.2	7.5	3.9
A_HTC_200_3	6.4	5.6	18.1	2.5	8.9	7.5	51.1	8.0	5.7
A_HTC_260_0.5	5.4	5.9	20.3	2.2	4.2	6.7	55.4	10.3	13.2
A_HTC_260_3	4.8	6.1	22.0	2.1	3.1	6.7	55.2	11.5	17.8
A_Py_600_1	6.0	10.8	68.5	4.2	3.3	1.8	5.4	0.9	1.6
T_SS	10.7	1.9	7.5	4.9	22.6	14.3	37.6	3.5	1.7
T_HTC_200_0.5	10.1	5.0	19.3	2.8	8.4	9.2	45.2	4.5	5.4
T_HTC_200_3	7.4	6.1	24.1	2.7	5.1	6.1	48.6	6.6	9.5
T_HTC_260_0.5	7.3	6.5	25.2	1.9	3.3	4.8	51.0	7.0	15.5
T_HTC_260_3	5.0	6.1	25.2	2.8	3.1	5.7	52.3	10.5	16.9
T_Py_600_1	5.8	12.1	68.6	4.9	2.8	1.3	4.5	0.8	1.6

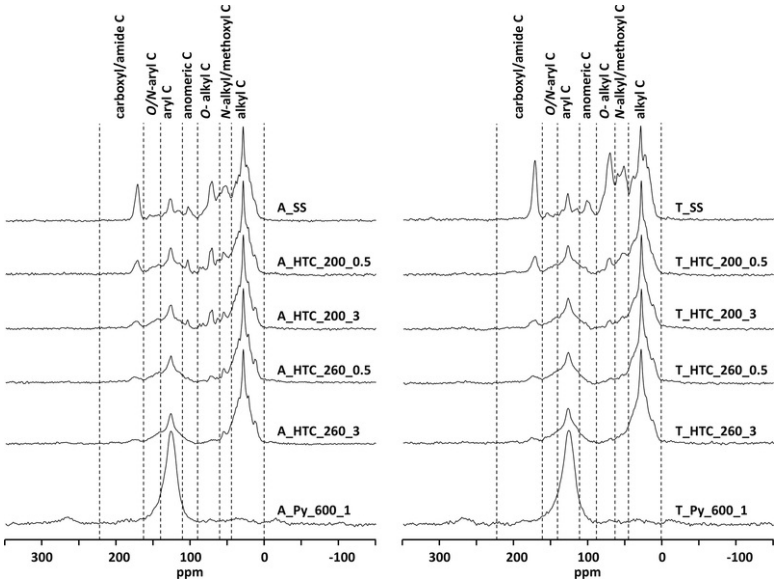

Fig. 2 Solid-state ^{13}C NMR spectra of primary (A_SS) and secondary (T_SS) sewage sludges and their respective hydrochars produced at 200 °C (_HTC_200) and 260 °C (_HTC_260) for 0.5 and 3 hours (_0.5, _3, respectively), as well as the pyrochars produced at 600 °C for 1 h (_Py__600_1).

alt-text: Fig. 2

Calculating the alkyl C/carboxyl C ratios from the intensity distribution of the ^{13}C NMR spectra as an index for the average chain length of the alkyl residues, values of 4.7 and 3.5 (Table 3) are obtained confirming that in our SS samples, lipids comprise a major fraction. This is in line with results by Jin-hong et al. [38]. The higher value of this ratio obtained for A_SS may be due to the anaerobic conditions during its production, which leads to a preferential preservation of long chain paraffinic structures. In addition, the higher N content of T_SS compared to A_SS is consistent with the higher ^{13}C-intensity in the region of *N*-alkyl C spectrum. This points to a higher proportion of proteinaceous material for the former than for the latter, which

contributes to decrease the alkyl C/carboxyl C ratio. Carbohydrates are commonly preferentially degraded during thermal treatments, leading to the relative enrichment of all other compound classes. Based on this, Baldock et al. [40] introduced the ratio alkyl C/*O*-alkyl C as an index for the degradation degree. Calculating this ratio, a value of 2.5 was obtained for A_SS and 1.7 for T_SS (Table 3), confirming that the material of the anaerobic pond (A) is more humified, thus biochemically stabilized, than that derived from the "thickener pond" (T).

The solid-state ^{15}N NMR spectra of both A_SS and T_SS are dominated by a signal at −260 ppm in the chemical shift region of amide N (from −248 to −285 ppm), Fig. 3. This signal contributes with 69 and 74% to the total ^{15}N intensity of the spectra of A_SS and T_SS, respectively (Table 5). Most of this nitrogen occurs as peptides and, to a lower amount, as amides in amino sugars. Note that some amide structures are also contributing to the shoulder between −230 and −248 ppm. The respective *N*-alkyl C of these compounds gives rise to signals in the chemical shift region between 60 and 45 ppm of the ^{13}C NMR spectra. This signal contributes with 13 and 14% to the total ^{13}C intensity of the spectra of A_SS and E_SS, respectively (Table 3). Although lignin is not considered as a major component of sewage sludge, its methoxyl C would contribute to the signal of this region, too. The peak at −346 ppm, which appears in both A_SS and T_SS ^{15}N NMR spectra, corresponds to free aliphatic amino groups of amino acids or amino sugars, but the low signal-to-noise ratios of the spectra does not allow an unbiased differentiation of such a signal from the noise. Regarding pyrrole compounds (from −150 to −248 ppm) A_SS shows a higher contribution, with a 22%, than T_SS with a 17% (Table 5). However, in contrast to Liu et al. [24] who applied X-ray photoelectron spectroscopy (XPS), no indications for the presence of pyridine N or nitrile N was evidenced. In studies about the nitrite fixation to humic material, their chemical shifts were found between −65 to −80 ppm and −90 to −140 ppm, respectively [39].

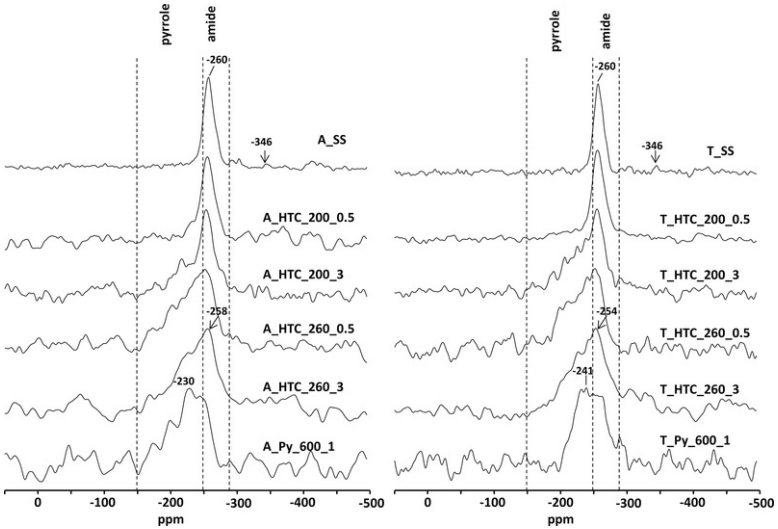

Fig. 3 Solid-state ^{15}N NMR spectra of primary (A_SS) and secondary (T_SS) sewage sludges and their respective hydrochars produced at 200 °C (_HTC_200) and 260 °C (_HTC_260) for 0.5 and 3 h~~ours~~ (_0.5, _3, respectively), as well as the pyrochars produced at 600 °C for 1 h (_Py__600_1).

alt-text: Fig. 3

3.2.2 Hydrochars and pyrochars

After HTC, the contribution of the chemical shift region of alkyl C to the total ^{13}C intensity increased for the A samples from 43 (A_SS) to 55% (260 °C, 30 min) and for the T set from 38 (T_SS) up to 52% (260 °C, 3 h) (Table 3). An augmentation in this region was also observed by Jin-hong et al. [38] after HTC of SS at 190 and 260 °C for 1 h. Table 4, showing the recovery of C in the different C groups after HTC treatment, indicates that there was no net-synthesis or degradation of lipids, but a relative enrichment due to the loss of other compounds. Thus, lipids were not affected by HTC, which is in line with previous works of Popov et al. [41] and Shin et al. [42]. The latter demonstrated that three kinds of fatty acids were stable under subcritical water conditions at temperatures of 300 °C or below.

Table 4 C-recovery of the different C groups of primary (A_SS) and secondary (T_SS) sewage sludges as a function of charring conditions (% of C present in the original sewage sludge).

alt-text: Table 4

	Carboxyl/amide C	*O/N*- Aryl C	Aryl C	*O*-Alkyl C	*N* Alkyl/Methoxyl C	Alkyl C

ppm	220–160	160–140	140–110	110–90	90–60	60–45	45–0
A_SS	9	3	10	4	17	13	43
A_HTC_200_0.5	5	4	14	3	10	8	40
A_HTC_200_3	5	5	15	2	7	6	42
A_HTC_260_0.5	4	5	16	2	3	5	43
A_HTC_260_3	4	5	17	2	3	5	44
A_Py_600_1	3	5	29	2	1	1	2
T_SS	11	2	8	5	23	14	38
T_HTC_200_0.5	8	4	15	2	7	7	36
T_HTC_200_3	6	5	18	2	4	5	37
T_HTC_260_0.5	5	5	18	1	2	3	35
T_HTC_260_3	3	4	17	2	2	4	35
T_Py_600_1	3	5	31	2	1	1	2

Table 5 Relative distribution of the ^{15}N intensity between the chemical shift region −150 to −285 ppm of the solid-state ^{15}N NMR spectra of primary (A_SS) and secondary (T_SS) sewage sludges and their respective hydrochars produced at 200 °C (_HTC_200) and 260 °C (_HTC_260) for 0.5 and 3 h~~ours~~ (_0.5, _3, respectively), as well as the pyrochars produced at 600 °C for 1 h (_Py__600_1).

alt-text: Table 5

	Pyrrole N	Amide N
ppm	−150 to −248	−248 to −285
A_SS	22.4	77.6
A_HTC_200_0.5	38.7	61.3
A_HTC_200_3	50.9	49.1
A_HTC_260_0.5	65.3	34.7
A_HTC_260_3	60.3	39.7
A_Py_600_1	75.4	24.6
T_SS	17.2	82.8
T_HTC_200_0.5	30.5	69.5
T_HTC_200_3	56.3	43.7
T_HTC_260_0.5	64.7	35.3
T_HTC_260_3	57.0	43.0
T_Py_600_1	58.2	41.8

As expected, HTC resulted in decarboxylation which is revealed by the diminishment of the recovery of C as carboxyl C. Whereas *O- and N*-alkyl C were degraded, as HTC charring temperature and time increased, aromatic C was formed, most

likely by dehydration and cyclization of carbohydrates and peptideous material. This is indicated by the increase of C which occurs as aryl C and *O*- and *N*-aryl C for both, the "A" and "T" hydrochars (Table 4). The latter suggests the formation of furans and N-heterocyclic aromatic structures. Jin-hong et al. [38] reported comparable results for SS hydrochars. Considering that O/N-aryl C constitutes a third of the aromatic C in the hydrochars, a predominantly polyfuran core with additional N-heterocyclic aromatic units instead of a benzoidal graphenic network (arene structures) has to be assumed [15]. As expected, an increase in the alkyl C/*O*-alkyl C ratio occurred after HTC. This increase was more affected by temperature than by time with HTC. The highest values were obtained for hydrochars produced at 260 °C for 3 h, with 17.8 and 16.9 for "A" and "T" hydrochars, respectively (Table 3).

Pyrolysis resulted in more drastic chemical changes, which are expressed in an almost complete transformation of organic matter into aromatic structures. In the spectra of A_Py_600_1 and T_Py_600_1, the aryl C region between 140 and 110 ppm accounts for 69% of the total ^{13}C intensity (Table 3) and the *O*- and *N*-aryl C region for only 11~~to~~12%, respectively. This can be taken as an indication that benzoic rings rather than furans dominate the aromatic network.

The ^{15}N NMR spectra of the hydrochars confirm the formation of N-heterocyclic aromatics during HTC already at 200 °C by a clear shoulder in the region of pyrrole-type N (~~−~~150 and −248 ppm). Structures such as indoles, imidazole and pyrroles are contributing to the intensity in this region. Protonated pyridine-type N may be a further component giving rise to intensity around this chemical shift but considering the pH of the samples, such structures are unlikely. However, unprotonated pyridine-type N may contribute to the weak shoulder around −70 ppm, but the low signal-to-noise ratios of the spectra does not allow an unbiased differentiation of such a signal from the noise. In contrast to the observations derived from ^{13}C NMR spectroscopy, the solid-state ^{15}N NMR spectra indicate chemical changes, expressed as an augmentation of the pyrrole-type N, not only with increasing temperature but also with residence time. The change is also expressed in a shift of the peak of the main signal from −260 ppm to −254 ppm. Note that pyrrole N has its chemical shift around −230 ppm and indole N around −245 ppm. The largest contribution of pyrrole-type N is evidenced in the samples obtained after heating at 260 °C for 30 min, with a 65% for A_HTC_260_0.5 and T_HTC_260_0.5 (Table 5). The ^{15}N intensity in the chemical shift region of amide N (~~−~~248 to −285 ppm) underwent a drastic decrease after HTC. This region dominates only the spectra of hydrochars produced at the mildest HTC conditions. Here, it has to be taken into account that carbazole N has its chemical shift around −262 ppm. Benzamide-type N has its resonance frequency at −275 ppm. Thus, such compounds are likely to contribute to the amide N region as well. Regarding dry pyrolysis, it resulted in a dominance of pyrrole-type N with a contribution of 75 and 58% for A_600_1 and E_600_1, respectively (Table 5). Here, the main peak occurs at −240 ppm~~ (Table 6)~~.

Table 6 Peak positions in the FT-IR spectra in the current study and proposed assignments.

alt-text: Table 6

Peak position (cm^{-1}).	Proposed assignment.
3700–3600	OH groups in the mineral matter.
3600–3300	OH bond in water, carboxyl and hydroxyl groups.
2925	aliphatic methylene band.
2855	aliphatic methylene band.
1655–1648	amide band I (C═O vibration).
1600	aromatic C═C vibrations.
1539	amide band II (N═H vibration).
1230	amide band III (C═N vibration).
1080	strech of phosphodiesters.
1030	Si═O═Si vibrations
797–785	out of plane NH wagging in amides and/or bending of the aromatic ring C═H bonds
below 600	M═X streching vibrations in both organic and inorganic halogens compounds (M-metal, X-halogen)

3.3 Fourier transform-infrared spectroscopy

All FT-IR spectra (Fig. 4) of the original SS, hydrochars and pyrochars exhibit several peaks around 3700–3600 cm^{-1}, which are attributable to vibration of OH groups in the mineral matter [36,43]. The most relevant bands and peaks as well as their proposed assignments are compiled in Table 6. The peaks appearing from 3600 cm^{-1} to 3300 cm^{-1} are assigned to stretching OH bond in water, carboxyl and hydroxyl groups [43]. All spectra show these two bands but their intensities decrease after the HTC and dry pyrolysis processes. In addition, all spectra exhibit an intense signal at 1030 cm^{-1} which can be caused by Si

—

O

—

Si vibrations [32,25] or by C

—

-O vibrations in polysaccharides. Silicate may derive from street run-offs which also enter the waste water systems or from residues of the sand used during the mechanical pre-treatment of the water-cleaning process. The increase of this band with temperature supports such an assignment to Si-O-Si vibration since partial combustion of organic matter during heating leads to a relative enrichment of mineral matter of the sample. The FT-IR spectra of the untreated SS (A_SS and T_SS) indicate a pattern, which can be assigned to microbial biomass. This is composed of distinct aliphatic methylene bands at 2925 and 2855 cm^{-1}, the amide band I (C

=

O vibration) at 1655–1648 cm^{-1}, the amide band II (N

—

H vibration) at 1539 cm^{-1}, the amide band III (C

=

N vibration) at 1230 cm^{-1} and the stretch of phosphodiesters at 1080 cm^{-1} [44]. However, the contribution of the Si

—

O stretching in the 1100–1000 cm^{-1} region cannot be overlooked. Additionally, one has to bear in mind that the amide I and III bands can be overlapped by the C

=

O vibration of the carboxylates and the C

—

O vibration of carboxylic acids, respectively. In the carbonized samples they may also contain contributions from pyrans and furans derived from heat-altered carbohydrates. In addition, the peak around 797–785 cm^{-1} which is visible in all spectra is attributable to out of plane NH wagging in amides and/or bending of the aromatic ring C

—

H bonds [43]. The bands appearing below 600 cm^{-1} are probably due to M

—

X stretching vibrations in both organic and inorganic halogens compounds (M-metal, X-halogen) [36].

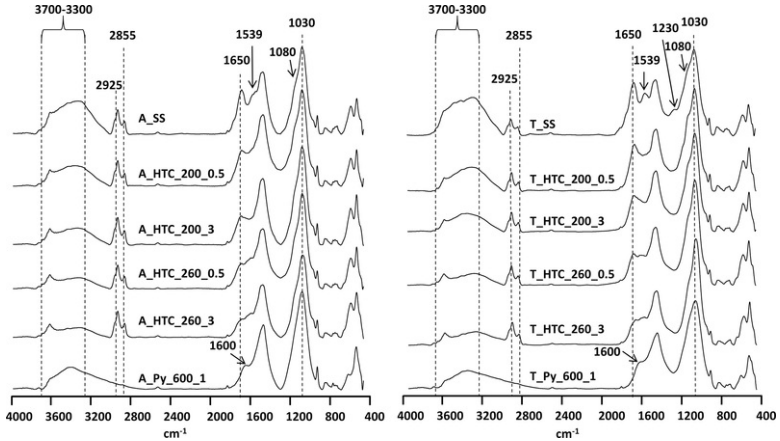

Fig. 4 FT-IR spectra of primary (A_SS) and secondary (T_SS) sewage sludges and their respective hydrochars produced at 200 °C (_HTC_200) and 260 °C (_HTC_260) for 0.5 and 3 hours (_0.5, _3, respectively), as well as the pyrochars produced at 600 °C for 1 h (_Py__600_1).

alt-text: Fig. 4

As already observed by solid-state NMR spectroscopy, HTC produced milder alterations of the FT-IR pattern as dry pyrolysis. Thus, the spectra of the hydrochars show the same peaks than those of the non-treated SS except for the lack of the amide II and III signals in the former. This is in line with the decrease of the amide N intensity in the ^{15}N NMR spectra as a result of the pyrolyzation process. In addition, the decrease of the FT-IR band corresponding to the OH vibrations derived from organic matter is in accordance with the loss of ^{13}C intensity in the O-alkyl C region. In addition, a new peak at 1600 cm^{-1} assigned to aromatic C

=

C vibrations appears in the spectra of the pyrochars. This may be interpreted that the higher temperatures resulted in a preferential accumulation of arene structures as it was also indicated by the respective solid-state ^{13}C NMR spectra. It is worth to notice that all inorganic signals are still present after dry pyrolysis whereas those assigned to aliphatic methylene (2925 and 2855 cm^{-1}), phosphodiester (1080 cm^{-1}) and amide I, II and III disappeared.

3.4 Summary of the main chemical alterations caused by thermochemical carbonization of sewage sludge samples

It is accepted that the degradation of biomass primarily initiates with a hydrolysis step at approximately 200° C during HTC, due to the increased vapor pressure [13,19]. Considering the main components of SS, hydrolysis will likely produce the cleavage of amide bond of proteins and the ether bond of carbohydrates, resulting in peptides, amino acids and monomeric sugars. Part of those compounds are dissolved in the reaction water and removed after HTC, contributing to the observed decline of total organic matter and of *O*- and *N*- alkyl C, carboxyl C but also of amide N after the HTC treatment. However, highly reactive products with low molecular weight are also formed which are likely to recondensate to form insoluble products which can precipitate. A further process represents dehydration, which removes water from the organic molecules leading to formation of aromatic structures. This was also observable in our experiment by the increase of C groups assigned to the ^{13}C chemical shift region between 160 and 110 ppm. Relating the C content adding to the intensity in the *O*- and *N*-alkyl C region (90–45 ppm) with that contributing to the aromatic C region (160–110 ppm) reveals high and negative correlation with R^2 = 0.95 for "A" samples and R^2 = 0.97 for "T" samples. The loss of carboxyl C during HTC confirms the occurrence of decarboxylation processes, although the detailed reaction mechanisms are largely unknown [13].

3.5 Potential as source of N for agriculture

The total N content has to be considered for both fast and slow-release N fertilization purposes. However, N_i contents are mostly important from a fast fertilization point of view. Total nitrogen losses increased with temperature and were higher for pyrolysis than for HTC. However, the organic N resisting in the chars occurs in forms which are expected to have higher biochemical recalcitrance than the N forms in the original feedstock. This is an observation which has to be considered if biochars/pyrochar and hydrochars are produced from N-rich feedstocks with the intention to use them as slow release fertilizer. Careful calculations are necessary if the thermally induced N-losses can compensate the N-losses occurring after direct application of the feedstock without thermal pretreatment. In the case of the latter, fast N-losses are expected if the N-mobilization from SS is faster than N-immobilization due to N-uptake by the growing plants. The highest total and inorganic N contents were obtained by using HTC at 200 °C for 30 min so such HTC chars will be preferable if fast fertilization at the beginning of the growing period is necessary. However, a key property of a slow-release N fertilizer is its N sequestration either by incorporation of N into compounds with low microbial accessibility or by N adsorption on the surface of the chars. Thus, the thermal transformation of peptides into N-containing heterocyclic aromatic compounds may be of higher value if such products are needed.

A further consideration lays in the observation recently made by [45]. They observed a higher increase of the microbial activity in soil amended with hydrochars than with biochars, which was explained with a higher content of biochemically labile compounds in the first if compared to the latter. Microbial growth is commonly connected to N-immobilization into newly synthetized microbial biomass, which represents an important sink for decreasing mineral-N concentrations in soils.

Besides the valuable retention and slow release of plant nutrients like nitrogen, it has to be taken into account that the HTC process may also form a variety of potentially harmful benzenic, phenolic and furanic volatiles along with various aldehydes and ketones [46]. These compounds formed in feedstock- and temperature-specific patterns are also found in the liquid and the solid phase of HTC chars. This problem may be handled by different post-treatments which remove these undesirable substances. As reported by Schulze et al. [47] readily available and fast-cycling carbon fractions can efficiently be separated from hydrochars by washing and fermentation.

Regarding the organic amendment potential of SS chars, carbon contents are below 250 mg g^{-1}, which does not justify to define this type of char as biochar [48,11] and which reflects its minor role in increasing the soil organic carbon content. However, other soil properties which have not been considered in this study may be improved. Compared to the analyzed HTC chars, our pyrochars may have a higher impact on increasing the carbon sequestration potential of soils due to their higher aromaticity and their lower content of oxygen or nitrogen substituted aromatic C.

Besides the sequestration of carbon, nitrogen and other nutrients, in particular of phosphate in the case of chars derived from SS, laboratory studies of Dicke et al. [49] demonstrated the potential of HTC chars to reduce N_2O emissions.

4 C~~ONCLUSIONS~~onclusions

Our study showed that peptide-like N of SS is transferred into heterocyclic aromatic N during heat treatment, although the efficiency of this transformation is different for pyrolysis and HTC. Former studies on N-rich charcoal confirmed that the N bound in this so-called black nitrogen can be used for plant growth as a kind of slow-N-release fertilizer [22]. However, the different contribution of various N-classes to the total N in hydrochars and pyrochars from SS, will affect their N fertilization capability. Based on the higher N_i content, the hydrochars produced at 200° for 30 min may be the most appropriate if both immediate and medium term N-fertilization is required, whereas the pyrochar may be useful if smaller N doses are needed over a longer time range. However, one has to bear in mind that pyrolysis results in high N loss due to volatilization. On the other hand, this N loss may be outbalanced by the

sequestration of the remaining N in heterocyclic forms, which increases the pool of organic N with medium-term biochemical recalcitrance. Nevertheless, both HTC and pyrolysis represent efficient tools for hygienization of SS.

Considering that SS is an organic waste, the N and P of which are lost if deposited on landfills or used for combustion as energy source, the transformation of this material into pyrochar or hydrochar for their use as soil amendment can be seen as an efficient tool to recycle N and P from organic waste.

Acknowledgements

This work was supported by the Spanish Ministry of Economy and Competitiveness (projects PCGL2012-37041, CGL2015-64811-P and CGL2016-76498-R) and the Spanish Ministry of Education, Culture and Sport (Marina Paneque FPU fellowship, FPU 13/05831). Carlos Aragón and the Experimental Wastewater Treatment plant (CENTA) are acknowledged for providing the sewage sludge samples. Dr. Ulf Lüder (Leibniz-Institut für Agrartechnik and Bioengineering, Potsdam (Germany)) is thanked for his assistance during the production of the chars. Marta Velasco-Molina (IRNAS-CSIC, Sevilla) is gratefully acknowledged for her technical assistance.

References

[1] WRAP (Waste and Resources Action Programme), UK. Organic Waste Market Situation Report- Realising the value of organic waste. http://www.wrap.org.uk/sites/files/wrap/Organics%20Market%20Situation%20Report%20Spring%202008.~~pdf~~pdf, 2008 (accessed 24.07.17).

[2] L.E. Sommers, Chemical composition of sewage sludges and analysis of their potential use as fertilizers, *J. Environ. Qual.* **6**, 1977, 225–232.

[3] J. Kern, B. Heinzmann, B. Markus, A.C. Kaufmann, N. Soethe and C. Engels, Recycling and assessment of struvite phosphorus from upgraded sewage sludge, *Agric~~ultural Engineering International: The CIGR Ejournal~~. Eng. Int. CIGR E-J.* **10**, 2008, CE1201.

[4] T.F.H. Theobald, M. Schipper and J. Kern, Phosphorus ~~F~~flows in Berlin-Brandenburg, a ~~Regional Flow A~~regional flow analysis, *Resour. Conserv. Recyc.* **112**, 2016, 1–14.

[5] M.J. Goss, A. Tubeileh and D. Goorahoo, A ~~R~~review of the use of organic amendments and the risk to human health, In: D.L. Sparks, (Ed), *Advances in Agronomy,* 2013, Cambridge, 277–348.

[6] J. Werther and T. Ogada, Sewage sludge combustion, *Prog. Energy Combust. Sci.* **25**, 1999, 55–116.

[7] Council Directive 1986/278/EEC, Council Directive 1986/278/EEC, of 12 June 1986 on the protection of the environment, and in particular of the soil, when sewage sludge is used in agriculture, *Off~~icial Journa~~l. J. L* **181**, 1986, 6–12.

[8] European Commission Working document on sludge. 3rd Draft. 27 April. ENV.E.3/LM. Brussels, Belgium. DG Environment, 2000.

[9] A. Kelessidis and A.S. Stasinakis, Comparative study of the methods used for treatment and final disposal of sewage sludge in European countries, *Waste Manage.* **32**, 2012, 1186–1195.

[10] J. Lehmann and S. Joseph, Biochar for Environmental Management: Science and Technology, second ed., 2015, Earthscan; London.

[11] European Biochar Foundation. European Biochar Certificate − Guidelines for a Sustainable Production of Biochar: Version 6.2 of 4th February 2016 [online]. Arbaz, Switzerland. Available from: http://www.european-biochar.org/biochar/media/doc/ebc-guidelines.pdf, 2012 (accessed 24.07.17).

[12] J. Libra, K. Ro, C. Kammann, A. Funke, N. Berge, Y. Neubauer, M. Titirici, C. Fuhner, O. Bens, J. Kern and K. Emmerich, Hydrothermal carbonization of biomass residuals: a comparative review of the chemistry, processes and applications of wet and dry pyrolysis, *Biofuels* **2**, 2011, 89–124.

[13] A. Funke and F. Ziegler, Hydrothermal carbonization of biomass: ~~A~~a summary and discussion of chemical mechanisms for process engineering, *Biofuels Bioprod. Biorefin.* **4**, 2010, 160–177.

[14] C. Falco, F.P. Caballero, F. Babonneau, C. Gervais, G. Laurent, M.M. Titirici and N. Baccile, Hydrothermal carbon from biomass: structural differences between hydrothermal and pyrolyzed carbons via ^{13}C solid state NMR, *Langmuir* **27**, 2011, 14460–14471.

[15] N. Baccile, G. Laurent, F. Babonneau, F. Fayon, M.M. Titirici and M. Antonietti, Structural ~~Characterization of Hydrothermal Carbon Spheres by Advanced S~~characterization of hydrothermal carbon spheres by advanced solid-State MAS ^{13}C NMR ~~I~~investigations, *J. Phys. Chem. C* **113**, 2009, 9644–9654.

[16] N. Baccile, G. Laurent, C. Coelho, F. Babonneau, L. Zhao and M.M. Titirici, Structural insights on ~~N~~nitrogen-containing hydrothermal carbon using solid-state magic angle spinning ^{13}C and ^{15}N nuclear magnetic resonance, *J. Phys. Chem. C* **115**, 2011, 8976–8982.

[17] X. Lu and N.D. Berge, Influence of feedstock chemical composition on product formation and characteristics derived from the hydrothermal carbonization of mixed feedstocks, *Bioresour. Technol.* **166**, 2014, 120–131

[18] M.T. Reza, M.H. Uddin, J.G. Lynam, S.K. Hoekman and C.J. Coronella, Hydrothermal carbonization of loblolly pine: reaction chemistry and water balance, *Biomass Conv. Bioref.* **4**, 2014, 311–321.

[19] M.T. Reza, B. Wirth, U. Lüder and M. Werner, Behavior of selected hydrolyzed and dehydrated products during hydrothermal carbonization of biomass, *Bioresour. Technol.* **169**, 2014, 352–361.

[20] H. Knicker, A. Hilscher, F.J. González-Vila and G. Almendros, A new conceptual model for the structural properties of char produced during vegetation fires, *Org. Geochem.* **39**, 2008, 935–939.

[21] H. Knicker, "Black nitrogen"- an important fraction in determining the recalcitrance of charcoal, *Org. Geochem.* **41**, 2010, 947–950.

[22] J.M. De la Rosa and H. Knicker, Bioavailability of N released from N-rich pyrogenic organic matter: an incubation study, *Soil Biol. Biochem.* **43**, 2011, 2368–2373.

[23] L. Wei, L. Wen, T. Yang and N. Zhang, Nitrogen transformation during sewage sludge pyrolysis, *Energy Fuels* **29**, 2015, 5088–5094.

[24] T. Liu, Y. Guo, N. Peng, Q. Lang, Y. Xia, C. Gai and Z. Li, Nitrogen transformation among char, tar and gas during pyrolysis of sewage sludge and corresponding hydrochar, *J. Anal. Appl. Pyrolysis* 2017, https://doi.org/10.1016/j.jaag.2017.05.017.

[25] A. Zielinska, P. Oleszczuk, B. Charmas, J. Skubiszewska-Zieba and S. Pasieczna-Patkowskaca, Effect of sewage sludge properties on the biochar characteristic, *J. Anal. Appl. Pyrolysis* **112**, 2015, 201–213.

[26] C.N. Gonçalves, R.S.D. Dalmolin, D.P. Dick, H. Knicker, E. Klamt and I. Kögel-Knabner, The effect of 10% HF treatment on the resolution of CPMAS ^{13}CNMR spectra and on the quality of organic matter in Ferralsols, *Geoderma* **116**, 2003, 373–392.

[27] E. Danso-Boateng, G. Shama, A.D. Wheatley, S.J. Martin and R.G. Holdich, Hydrothermal carbonisation of sewage sludge: ~~E~~effect of process conditions on product characteristics and methane production, *Bioresour. Technol.* **177**, 2015, 318–327.

[28] H. Knicker, K.U. Totsche, G. Almendros and F.J. González-Vila, Condensation degree of burnt peat and plant residues and the reliability of solid-state VACP MAS ^{13}C NMR spectra obtained from pyrogenic humic material, *Org. Geochem.* **36**, 2005, 1359–1377.

[29] D.B. Wiedemeier, S. Abiven, W.C. Hockaday, M. Keiluweit, M. Kleber, C.A. Masiello, A.V. McBeath, P.S. Nico, L.A. Pyle, P.W. Maximilian, M.P.W. Schneider, R.J. Smernik, G.L.B. Wiesenberg, W.I. Michael and M.W.I. Schmidt, Aromaticity and degree of aromatic condensation of char, *Org. Geochem.* **78**, 2015, 135–143.

[30] M. Sevilla, J.A. Maciá-Agulló and A.B. Fuertes, Hydrothermal carbonization of biomass as a route for the sequestration of CO_2: ~~C~~chemical and structural properties of the carbonized products, *Biomass Bioenergy* **35**, 2011, 3152–3159.

[31] J.M. De la Rosa, M. Paneque, A.Z. Miller and H. Knicker, Relating physical and chemical properties of four different biochars and their application rate to biomass production of Lolium perenne on a Calcic Cambisol during a pot experiment of 79 days, *Sci. Total Environ.* **499**, 2014, 175–184.

[32] C. Peng, Y. Zhai, Y. Zhu, B. Xu, T. Wang, C. Li and G. Zeng, Production of char from sewage sludge employing hydrothermal carbonization: ~~C~~char properties, combustion behavior and thermal characteristics, *Fuel* **176**, 2016, 110–118.

[33] J. Porta, M. López-Acevedo and C. Roquero, Edafología para la agricultura y el medio ambiente, third ed., 2003, Mundi-Prensa; Madrid.

[34] P. Alvarenga, C. Mourinha, M. Farto, T. Santos, P. Palma, J. Sengo, M.C. Morais and C. Cunha-Queda, Sewage sludge, compost and other representative organic wastes as agricultural soil amendments: ~~B~~benefits *versus* limiting factors, *Waste Manage.* **40**, 2015, 44–52.

[35] H.G. Adegbidi and R.D. Briggs, Nitrogen mineralization of sewage sludge and composted poultry manure applied to willow in a greenhouse experiment, *Biomass Bioenergy* **25**, 2003, 665–673.

[36] M.K. Hossain, V. Strezov, K.Y. Chan, A. Ziolkowski and P.F. Nelson, Influence of pyrolysis temperature on production and nutrient properties of wastewater sludge biochar, *J. Environ. Manage.* **92**, 2011, 223–228.

[37] M. Sohn and C.T. Ho, Ammonia ~~Generation during Thermal Degradation of Amino A~~generation during thermal degradation of amino acids, *J. Agric. Food Chem.* **43**, 1995, 3001–3003.

[38] Z. Jin-hong, L. Qi-mei and Z. Xiao-ron, The hydrochars characters of municipal sewage sludge under different hydrothermal temperatures and durations, *J. Integr. Agric.* **13**, 2014, 471–482.

[39] K.A. Thorn and L.G. Cox, Nitrosation and ~~Nitration of Fulvic Acid, Peat and Coal with Nitric AcidPLoS ONE~~nitration of fulvic acid, peat and coal with nitric acid, *PLoS One* **11**, 2016, e0154981.

[40] J.A. Baldock, J.M. Oades, P.N. Nelson, T.M. Skene, A. Golchin and P. Clarke, Assessing the extent of decomposition of natural organic materials using solid-state ^{13}C NMR spectroscopy, *Aust. J. Soil Res.* **35**, 1997, 1061–1083.

[41] S. Popov, T. Abdel-Fattah and S. Kumar, Hydrothermal treatment for enhancing oil extraction and hydrochar production from oilseeds, *Renew. Energy* **85**, 2016, 844–853.

[42] H.Y. Shin, J.H. Ryu, S.Y. Park and S.Y. Bae, Thermal stability of fatty acids in subcritical water, *J. Anal. Appl. Pyrolysis* **98**, 2012, 250–253.

[43] M.H. Bernier, G.J. Levy, P. Fine and M. Borisover, Organic matter composition in soils irrigated with treated wastewater: FT-IR spectroscopic analysis of bulk soil samples, *Geoderma* **209–210**, 2013, 233–240.

[44] E. Smidt and V. Parravicini, Effect of sewage sludge treatment and additional aerobic post-stabilization revealed by infrared spectroscopy and multivariate data analysis, *Bioresour. Technol.* **100**, 2009, 1775–1780.

[45] I. Bargmann, R. Martens, M.C. Rillig, A. Kruse and M. Kucke, Hydrochar amendment promotes microbial immobilization of mineral nitrogen, *J. Plant Nutr. Soil Sci.* **177**, 2014, 59–67.

[46] R. Becker, U. Dorgerloh, M. Helmis, J. Mumme, M. Diakite and I. Nehls, Hydrothermally carbonized plant materials: ~~P~~patterns of volatile organic compounds detected by gas chromatography, *Bioresour. Technol.* **130**, 2013, 621–628.

[47] M. Schulze, J. Mumme, A. Funke and J. Kern, Effects of selected process conditions on the stability of hydrochar in low-carbon sandy soil, *Geoderma* **257**, 2016, 137–145.

[48] S. Meyer, L. Genesio, I. Vogel, H.P. Schmidt, G. Soja, E. Someus, S. Shackley, F.G.A. Verheijen and B. Glaser, Biochar standardization and legislation harmonization, *J. Environ. Eng. Landsc.* **25**, 2017, 175–191.

[49] C. Dicke, G. Lanza, J. Mumme, R. Ellerbrock and J. Kern, Effect of hydrothermally carbonized char application on trace gas emissions from two sandy soil horizons, *J. Environ. Qual.* **43**, 2014, 1790–1798.

Highlights

- Thermochemical carbonization of sewage sludge leads to Pyrogenic organic Nitrogen formation.
- Hydrothermal carbonization (HTC) leads to polyfurans and dry pyrolysis to a benzoidal network.
- Temperature is more relevant than residence time for the structure of HTC.
- Nitrogen preservation was higher after HTC than after dry pyrolysis.
- Inorganic nitrogen (Ni) increased after HTC but was completely absent after dry pyrolysis.

Queries and Answers

Query: The author names have been tagged as given names and surnames (surnames are highlighted in teal color). Please confirm if they have been identified correctly.
Answer: Yes

Query: Please check the hierarchy of the section headings and correct if necessary.
Answer: Hierarchy is okey

Query: “Your article is registered as a regular item and is being processed for inclusion in a regular issue of the journal. If this is NOT correct and your article belongs to a Special Issue/Collection

please contact j.mohideen@elsevier.com immediately prior to returning your corrections.”

Answer: Article is fine registered as a regular item and included in a regular issue of the journal

Query: Please note that Table 6 was not cited in the text. Please check that the citations suggested by the copyeditor are in the appropriate place, and correct if necessary.

Answer: We removed the citation suggested by the copyeditor since Table 6 belongs to the section number "3.3 Fourier transform-infrared spectroscopy". We added a new sentence to cite Table 6. In fact, table 6 should be moved to section 3.3 of the manuscript

Query: One or more sponsor names and the sponsor country identifier may have been edited to a standard format that enables better searching and identification of your article. Please check and correct if necessary.

Answer: Yes

Query: Please check the presentation of all the Tables and correct if necessary.

Answer: The values (numerical characters) contained in the tables 1, 2, 3, 4 and 5 appear shifted towards the left side in this proof version. They all should appear in the middle of the cell, like in the the example we atached. Table 6 is okey like that.